Monitoring of observation errors in the assimilation of satellite ozone data

Ivanka Stajner,[1] Nathan Winslow,[2] Richard B. Rood,[3] and Steven Pawson[4]

Global Modeling and Assimilation Office, NASA Goddard Space Flight Center, Greenbelt, Maryland, USA

[1] Ozone observations from the Solar Backscatter UltraViolet/2 (SBUV/2) instruments and/or the Earth Probe Total Ozone Mapping Spectrometer (EP TOMS) have been assimilated in near-real time at NASA's Data Assimilation Office (DAO) since January 2000. The ozone data assimilation system was used as a tool for detecting and characterizing changes in the observation errors. The forecast model captures the geophysical variability. A change in the observed-minus-forecast (O-F) residuals, which are defined as differences between the incoming ozone observations and the collocated short-term model forecast, indicates a change in the assimilation system. If the model and the statistical analysis scheme are stable, then it points to a modification in instrument characteristics or a retrieval algorithm. However, sometimes a change in the ozone O-F residuals is caused by differences in the availability of the meteorological observations or modifications in the meteorological assimilation system whose winds are used to drive the ozone transport model. The O-F residuals are routinely produced and monitored in the assimilation process. Using examples from the NOAA 14 and NOAA 16 SBUV/2 instruments, and the EP TOMS, we demonstrate that the monitoring of time series of O-F residual statistics is an effective, sensitive, and robust method for identifying time-dependent changes in the observation-error characteristics of ozone. In addition, the data assimilation system was used to assist in the validation of updated calibration coefficients for the NOAA 14 SBUV/2 instrument. This assimilation-based monitoring work is being extended to ozone data from instruments on new satellites: Environmental satellite (Envisat), Earth Observing System (EOS) Aqua, and EOS Aura.   *INDEX TERMS:* 0341 Atmospheric Composition and Structure: Middle atmosphere—constituent transport and chemistry (3334); 3337 Meteorology and Atmospheric Dynamics: Numerical modeling and data assimilation; 3360 Meteorology and Atmospheric Dynamics: Remote sensing; 3394 Meteorology and Atmospheric Dynamics: Instruments and techniques; *KEYWORDS:* assimilation, satellite, ozone data

1. Introduction

[2] Satellite borne instruments provide a wealth of data about the Earth's atmosphere with a continuous and often near-global coverage. A few examples are the TIROS Operational Vertical Sounder (TOVS) [*Smith et al.*, 1979], the Atmospheric Infrared Sounder (AIRS) [*Aumann et al.*, 2003], and the Total Ozone Mapping Spectrometer (TOMS) [*McPeters et al.*, 1998]. Satellite data are core input data sets with ever increasing importance for modern data assimilation systems. These systems are used to provide estimates and forecasts of the state of the atmosphere. Improvements in the availability, accuracy, and assimilation of satellite data are major factors contributing to the improvement in the accuracy of weather forecasts [*Hollingsworth et al.*, 2003]. Careful monitoring of the errors in the satellite data is critical for their optimal usage within assimilation systems. Improvements in understanding of satellite data and their errors contribute to increased accuracy of weather and atmospheric constituent forecasts, potentially enable improvements in forecast models, and can ultimately lead to a better understanding of the underlying geophysical processes.

[3] Validation of retrieved data from satellite borne instrument measurements is a difficult task that can be complicated by many factors [e.g., *Fetzer et al.*, 2003]. For newer instruments with high spectral and fine spatial resolution, such as AIRS, the large data volume makes the validation a very demanding task. Thus development and use of sensitive, automated procedures that can aid in the

---
[1]Science Applications International Corporation, Beltsville, Maryland, USA.

[2]Decision Systems Technologies, Inc., Rockville, Maryland, USA.

[3]Earth and Space Data Computing Division, NASA Goddard Space Flight Center, Greenbelt, Maryland, USA.

[4]Goddard Earth Sciences and Technology Center, University of Maryland Baltimore County, Baltimore, Maryland, USA.

monitoring and validation of retrieved satellite data is desirable.

[4] Traditionally, retrieved data products from satellite instruments have been validated in several ways. For example, algorithms used for their derivation are checked using synthetic and test input data [e.g., *Froidevaux et al.*, 1996]. Raw satellite-instrument radiances are monitored for abrupt changes and longer-term drifts. Zonal means of retrieved geophysical fields may be compared with the zonal means of model or assimilated fields [e.g., *Gille et al.*, 1996]. The retrieved products are compared to data from the same instrument and from different instruments [e.g., *Froidevaux et al.*, 1996; *Remsberg et al.*, 2002]. These comparisons are typically done using collocated data that are taken within certain distance and time from each other. The role of the collocation is to minimize the underlying temporal and spatial variability of geophysical fields. However, this dynamical variability is explicitly represented by the assimilated geophysical fields. This is one of the advantages of using assimilated fields in the validation of satellite data products.

[5] Data assimilation can contribute to validation of satellite data products. This approach capitalizes on the inherent ability of assimilation to handle large data volumes, often in near-real time, and facilitate a rapid feedback about the data quality to the instrument teams. Fields produced by assimilation into global models can provide a precise time and spatial collocation with every satellite measurement. The global nature of these fields allows application of averaging kernels, and production of a validation data set whose spatial representation is suitable for comparison with retrieved data. This is particularly important for instruments providing total or weighted columns of chemical constituents [e.g., *Rodgers and Connor*, 2003].

[6] Data assimilation techniques have been applied to monitoring and validation of observation errors. The framework was established by *Hollingsworth et al.* [1986], who demonstrated the value of data assimilation systems for monitoring of the performance of the radiosonde network. Long-term monitoring in meteorological reanalyses is presented by *Uppala* [1997], who demonstrated clear changes in system O-F biases for the radiosonde record and 1d-var retrievals of TOVS data over the period 1979–1993. *Piters et al.* [1999] validated Global Ozone Monitoring Experiment (GOME) total column ozone observations using the Assimilation Model at the Royal Dutch Meteorological Institute (KNMI). They evaluated a random error in GOME and found a systematic error depending on the viewing direction. Similar approaches have also been successfully used in calibration and validation of other types of satellite observations. *Stoffelen* [1999] used wind fields from a numerical weather prediction model in calibration of the European Remote Sensing Satellite (ERS) scatterometers. This calibration is beneficial to the ERS geophysical product (the surface wind field over oceans). It is used for monitoring of the ERS scatterometers, and it can detect sudden instrument anomalies within six hours. *Atlas et al.* [1999] performed geophysical validation of NASA scatterometer (NSCAT) data sets. They compared NSCAT data with collocated wind data from ships, buoys, other satellite date, and reference analyzed fields produced by assimilation of other data. These comparisons yielded estimates of the
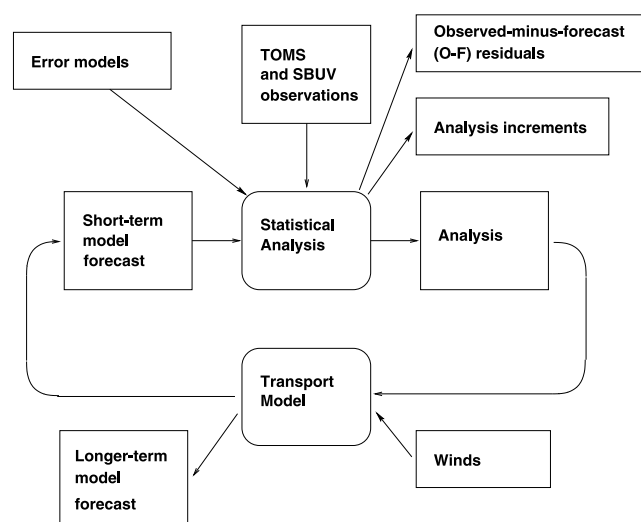
Figure 1. Schematic diagram of the ozone assimilation system with the major components and the data flow.

error characteristics of NSCAT data. When NSCAT data were assimilated, they found improvements in the resulting analysis and forecast fields.

[7] In this paper we apply data assimilation techniques to monitoring of the error characteristics of satellite ozone data. In section 2 we give a brief overview of the data assimilation system and of the techniques for monitoring of observation errors that are used throughout the paper. Subsequent sections contain examples from near-real time monitoring of errors in ozone data from three satellite-borne ozone instruments: the NOAA 14 Solar Backscatter Ultraviolet/2 (SBUV/2) instrument, the Earth Probe (EP) TOMS, and the NOAA 16 SBUV/2 instrument. In section 3 we focus on the changes in the NOAA 14 SBUV/2 ozone profile data error characteristics, and their impact on the assimilated ozone fields. Monitoring of total column ozone from EP TOMS and NOAA 16 SBUV/2 instruments is given in section 4. This section also includes examples of discontinuities in the O-F residual statistics due to changes in the meteorological data assimilation system. The use of global and regional statistics of the O-F residuals is illustrated by several examples of algorithm and calibration modifications in the NOAA 16 SBUV/2 ozone profiles in section 5. Discussion of the results and plans for future work are given in section 6.

2. Background

[8] Data assimilation [*Daley*, 1991] provides a framework for combining available observational atmospheric data, along with their error characteristics, with a model prediction and its error characteristics to obtain the best estimate of the true atmospheric fields. This process yields analyzed or assimilated fields. In the sequential ozone assimilation process used in this paper (see Figure 1) the model transfers information from previous observational times to the current synoptic time. At the new synoptic time the model estimated field is updated with observations. In regions with dense observations the model estimate is, perhaps, changed substantially. In regions with

sparse, or no, observations the estimate of the atmospheric field is largely determined by the model prediction. A statistical analysis scheme is used to produce an analysis field by combining the forecast field with the observations valid at this time according to their error characteristics. The cycle is then repeated. The forecast model can also be used to provide forecast fields for several days in advance. Data assimilation has been used successfully in numerical weather prediction, and increasingly also for obtaining distributions of atmospheric chemical constituents [e.g., *Austin*, 1992; *Fisher and Lary*, 1995; *Long et al.*, 1996; *Levelt et al.*, 1998; *Eskes et al.*, 1999; *Khattatov et al.*, 2000; *Ménard et al.*, 2000; *Elbern and Schmidt*, 2001; *Stajner et al.*, 2001; *Struthers et al.*, 2002; *Dethof and Holm*, 2002; *Eskes et al.*, 2003].

[9] An integral part of the data assimilation process is the computation of differences between the observations and the collocated model predictions of these quantities

$$\mathbf{w^o} - H\mathbf{w^f}, \tag{1}$$

where $\mathbf{w^o}$ is the vector of all the observations available at a single analysis time, H is the matrix of the observation operator, and $\mathbf{w^f}$ is the vector of the model forecast on the analysis grid. These differences are the vectors of the observed-minus-forecast (O-F) residuals, and they allow us to evaluate how consistent the observations are with our understanding of the atmosphere as described by the forecast model. Note that the observation error consists of the measurement or retrieval error and the representativeness error due to variability of the true field at scales that are unresolved by the discrete model. An O-F residual equals the difference between the observation error and the error in the forecast of the observed quantity. Thus the statistics of O-F residuals provide information about the observation and forecast errors. The O-F statistics are used extensively in data assimilation to monitor error characteristics and estimate error model parameters. For examples of their application in constituent data assimilation, see *Ménard et al.* [2000] and *Ménard and Chang* [2000]. Under the assumption that the forecast model does not change, and its error characteristics are constant in time, the differences in the time series of the O-F statistics are due to changes in the observation error characteristics. This approach that uses the forecast as a standard against which observations are compared has inherent advantages and disadvantages due to the underlying properties of assimilated fields. Advantages are that the forecast takes into account realistic geophysical variability of the true fields, and that global forecasts provide precise collocation with any observation. A disadvantage is that spatial and temporal variability of forecast errors complicates partitioning of the variability in O-Fs into the variability in forecast and observation errors, respectively. Implications for this work will be discussed below.

[10] This study uses near-real-time O-F residuals produced by the operational Goddard Earth Observing System (GEOS) ozone assimilation system [*Riishøjgaard et al.*, 2000; *Stajner et al.*, 2001]. The assimilated ozone fields agree well with independent high quality ozone data. See *Stajner et al.* [2001] for some examples of the comparisons of assimilated ozone against WMO ozone

sondes and Halogen Occultation Experiment (HALOE) [*Brühl et al.*, 1996]. In the initial configuration of the near-real time ozone assimilation system, the EP TOMS total column ozone [*McPeters et al.*, 1998] and the NOAA 14 SBUV/2 instrument ozone profiles [*Bhartia et al.*, 1996] were assimilated into a tracer transport model between January 2000 and April 2001. During April and May 2001 EP TOMS total column ozone and NOAA 16 SBUV/2 profile observations were assimilated. Only NOAA 16 SBUV/2 ozone total column and profile observations were assimilated from May 2001. The tracer transport model [*Lin and Rood*, 1996], which was used to predict ozone, was driven by the assimilated wind fields from the version 3 of the GEOS Data Assimilation System (DAS). Note that several operational changes were introduced into GEOS-3 during this period: their impacts will be discussed below.

[11] The GEOS ozone assimilation system produces time series of O-F statistics. We routinely monitor these time series for abrupt changes. We use global and regional mean and root-mean square (RMS) of O-F residuals for each data type. For profile observations these statistics are computed for each level. Another global statistic that we use in the monitoring is χ^2, defined as follows. If the errors in $\mathbf{w^o}$ and $\mathbf{w^f}$ are mutually uncorrelated Gaussian-distributed random vectors with mean 0 and covariances P and R, respectively, then the O-F residuals $\mathbf{w^o} - H\mathbf{w^f}$ are Gaussian distributed with the mean 0 and the covariance matrix $HPH^T + R$. The random variable

$$z = \left(\mathbf{w^o} - H\mathbf{w^f}\right)^T \left(HPH^T + R\right)^{-1} \left(\mathbf{w^o} - H\mathbf{w^f}\right), \tag{2}$$

then has the χ^2 distribution with p degrees of freedom, where p is the number of observations (dimension of $\mathbf{w^o}$) at one analysis time. The mean of z is p and the variance is $2p$. The mean of the normalized variable z/p is 1. Note that the representativeness error for TOMS total column data, whose footprint is smaller than the analysis model grid, is included as an additive component in the model used to evaluate R [*Stajner et al.*, 2001]. The SBUV footprint is comparable to the horizontal resolution of the analysis grid: thus the SBUV representativeness error need not be modeled explicitly. Initially, the χ^2 was monitored to check how consistent the assumed error covariance models are with the realizations of the O-F residuals. However, we found that χ^2 is also convenient for detecting changes in the observation error characteristics (as will be illustrated in section 5).

3. NOAA 14 Solar Backscattered Ultraviolet/2 (SBUV/2) Ozone Profiles

[12] Ozone profiles retrieved from NOAA 14 SBUV/2 instrument measurements and TOMS total ozone column data were assimilated in near-real time into the GEOS ozone system during the period between January 2000 and April 2001. The SBUV/2 instrument data are reported as partial ozone columns in 12 layers [*Bhartia et al.*, 1996]. Each of the layers 2 to 11 is ~5 km thick. Ozone partial columns from layers 3 (63–126 hPa) to 12 (0–0.25 hPa) are assimilated in our system [*Stajner et al.*, 2001]. In this section we focus on two examples of changes in NOAA 14 SBUV/2 error characteristics that can be seen from statistics
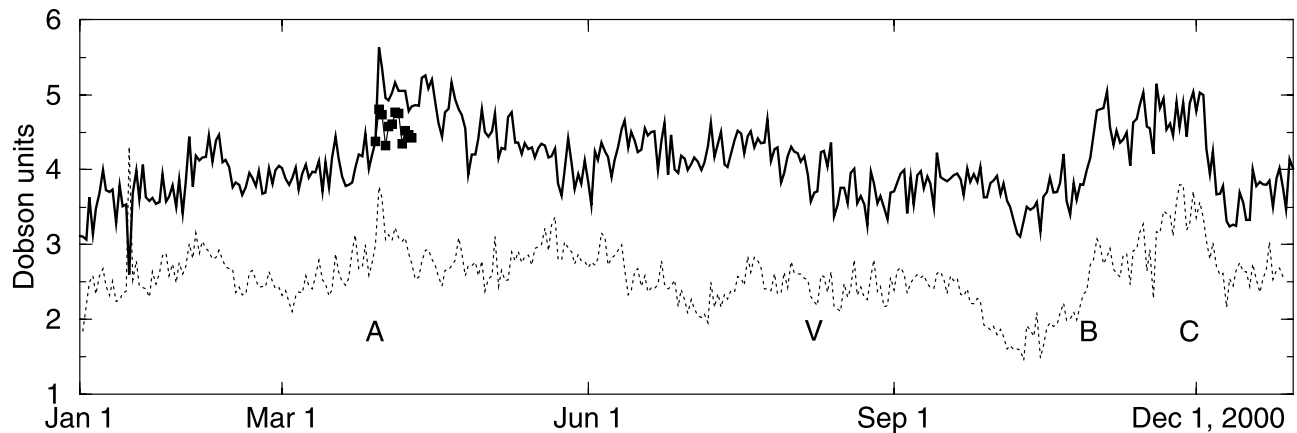
Figure 2. Time series of daily global mean of NOAA 14 SBUV/2 O-F residuals in Umkehr layer 5 for operational SBUV/2 data (solid line) is shown for the system driven by GEOS-3 winds. The same quantity from the ozone assimilation driven by winds from a prototype GEOS-4 system, and including parameterized ozone chemistry is shown by the dotted line. Note the sharp jump near the mark "A" exceeding the typical day-to-day variability followed by a downward trend in the mean of O-F residuals. This feature is coincident with the instrument calibration change on March 31. Near the mark "A" the same quantity is shown for assimilation driven by GEOS-3 winds and using reprocessed SBUV/2 data (line with squares). An increase between marks "B" and "C" coincides with a change in the grating position of the instrument.

of O-F residuals. We also examine impacts of changes in the formulation of the forecast model.

3.1. Features of the Data

[13] In order to evaluate temporal changes in the incoming SBUV/2 data we examine time series of statistics of O-F residuals. An example of the time series of the daily global mean of O-F residuals for NOAA 14 SBUV/2 in the layer 5, between 16 and 32 hPa, is shown by the solid line in Figure 2. For reference, an average of SBUV observations in this layer is ∼60 to 70 DU. Throughout the O-F mean time series there is a typical day-to-day variability of ∼0.5 DU. However, there is a sharp increase on March 31, 2000 (mark "A" in Figure 2). The forecast model did not change in any way on that day, but the calibration of the SBUV/2 instrument was modified. After the SBUV instrument team reexamined the calibration coefficients, they derived updated coefficients and reprocessed the data (M. Deland and D. McNamara, personal communication, 2000). We used the reprocessed SBUV/2 data in a short assimilation run, and the change in the global mean O-F value on March 31 was reduced. These later calibration coefficients were operationally implemented by NOAA on August 8, 2000, when the mean of O-F residuals slightly decreases (mark "V" in Figure 2).

[14] The second feature that stands out in the time series of the mean of O-F residuals in Figure 2 is the increase in November 2000 between marks "B" and "C". This period coincides with the changes in the NOAA 14 SBUV/2 instrument grating positions. When a grating position changes, the wavelength at which the measurement is made differs from the nominal wavelength, and the actual wavelength is also reported with less accuracy. The wavelength shift to a less optimal region of the spectrum, together with a less accurate knowledge of the actual wavelengths at which measurements are made, can increase the errors in the ozone retrieval from SBUV data. The larger O-F residuals indicate that there was indeed a change in the

quality of the SBUV/2 data simultaneous with the grating position changes.

3.2. Sensitivity to Forecast Model

[15] Next, we examine how robust are features in the time series of the O-F residual statistics to changes in the formulation of the forecast model. The time series of the global mean O-F residuals for NOAA 14 SBUV/2 data in layer 5 from an ozone assimilation into a modified ozone forecast model is shown by the dotted line in Figure 2. This model is driven by winds from a prototype of the version 4 of GEOS meteorological assimilation, and it includes a chemistry scheme with parameterized ozone production and loss rates [*Fleming et al.*, 2001], where production rates were adjusted so that the quotient of production and loss rates in the upper stratosphere agrees with an ozone climatology based on SBUV data [*Langematz*, 2000]. In contrast, the operational assimilation driven by GEOS-3 fields (solid line in Figure 2) does not include any chemistry, only the ozone transport, in the forecast model. Another difference between the operational GEOS-3 and prototype GEOS-4 meteorological systems is that the configuration of the operational system was changed a couple of times during year 2000, but a fixed version of the prototype GEOS-4 system was used for the entire year. The largest contribution to the mean differences between observations and forecasts comes from the tropical region. Both, upwelling and horizontal mixing reduce the ozone concentration in the SBUV/2 layer 5, just below the absolute mixing ratio peak near 10 hPa in the tropics. In the chemical parameterization, which is included in GEOS-4 driven ozone assimilation, there is net ozone production in this region. Thus the mean differences between observations and forecast in SBUV/2 layer 5 are smaller by ∼1.5 DU in the GEOS-4 driven assimilation. Comparisons of GEOS-4 driven assimilations with and without chemical parameterizations for the year 1998 indicate that ∼1 DU of this mean difference in SBUV/2 layer 5
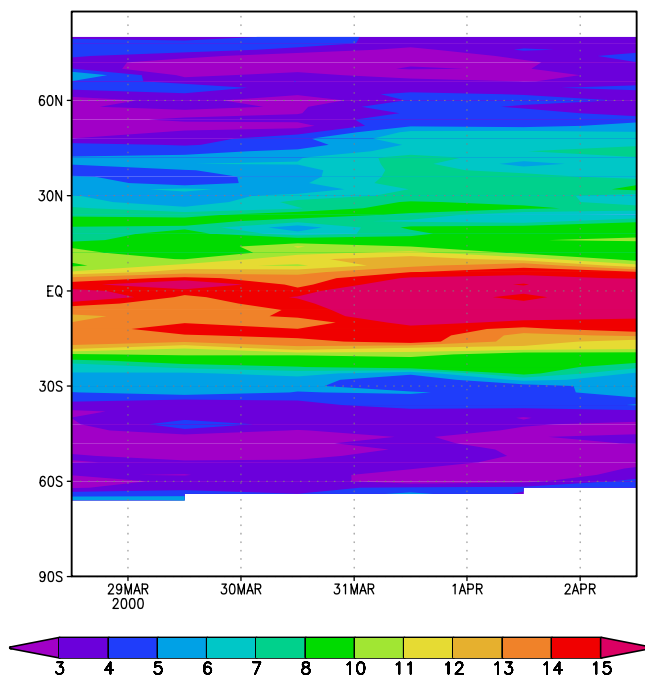
Figure 3. Zonal RMS of the differences between SBUV/2 observations and forecast of ozone column (in Dobson units) between 16 and 32 hPa (Umkehr layer 5) is shown during the period of the sharp increase in the global mean differences near mark "A" in Figure 2. The RMS differences increased most notably on March 31 in the Tropics and around 50°N to 60°N.

O-F residuals is due to chemistry. However, despite the offset between the O-F statistics from GEOS-3 and GEOS-4 driven assimilations in year 2000, the features arising from the changes in the SBUV/2 data (near mark "A" and between marks "B" and "C") are robust, and can be seen in both GEOS-3 and GEOS-4 time series.

3.3. Comparison of Changes in O-F Residuals, Observations, and Assimilated Fields

[16] In this section we compare the size of changes in the O-F residuals with the size of corresponding changes in the observations, and in the analyzed ozone fields. In our assimilation system both the forecast and the observation errors are assumed to have zero mean. If there is a modification of observation error characteristics that changes the mean of the observation errors, then assimilation of these observations will also change the mean of the analyzed ozone field. The size of the change will however depend on the forecast and observation error covariance models that are used in the assimilation.

[17] Statistics of O-F residuals can be very sensitive indicators of changes in observational error characteristics. Even though changes in zonal or global means of the observations can be relatively small, relative changes in O-F residuals can be easily noticeable. For example, the SBUV/2 calibration change on March 31, 2000 increased the zonal mean of ozone by ~1–2%, but the change in O-F residuals was ~10%. The latitudinal distribution of the impact of this SBUV/2 calibration change is seen in Figure 3. The zonal RMS of SBUV O-F residuals increase

throughout the tropics and in the northern middle latitudes. Most marked increase is seen near the equator and around 50°N to 60°N. There is almost no impact in the northern high latitudes or southern middle latitudes. Largest increases in the O-F RMS are seen where there are largest jumps in the zonal mean of the SBUV retrieved ozone between March 30 and 31. One exception is in the northern high latitudes between 75°N and 80°N. The zonal mean of SBUV ozone increased substantially by ~3 DU, but the RMS of O-F residuals was slightly improved. This reduction in the RMS may be due to a decrease of the meridional gradient in the zonal mean of the retrieved ozone. Zonal means of the retrieved ozone in two degrees wide latitude bands in the region between 70°N and 80°N vary by ~6 DU on March 30, but only by <2 DU on March 31.

[18] We now examine statistical significance of the changes in the observation means between March 30 and 31 at the level of significance of 1%. The change in the global mean of the observations between March 30 and 31 is about $\mu = 1.2$ DU, the standard deviations for observations on these days are $\sigma_1 = 8.936$ and $\sigma_2 = 9.292$ DU with $N_1 = 1142$ and $N_2 = 925$ observations per day, respectively. In order to test the hypothesis that the population means are equal [e.g., Spiegel, 1975], we evaluate the standardized variable

$$Z = \mu/\text{sqrt}(\sigma_1^2/N_1 + \sigma_2^2/N_2), \quad (3)$$

which for these samples equals 2.969. The critical region for a two-tailed test is outside the interval between the critical values −2.58 and 2.58, because 99% of the area under the standard normal curve is between these critical values. The computed value of Z is in the critical region, and thus we reject the hypothesis that the means are equal at a 1% level of significance.

[19] We will reuse the same notation for computation of statistical significance of the change in the O-F mean. The change in the global mean of the O-F residuals between March 30 and 31 is about $\mu = 1.254$ DU, the standard deviations for observations on these days are $\sigma_1 = 6.259$ and $\sigma_2 = 6.265$ DU with $N_1 = 1142$ and $N_2 = 925$ O-F residuals per day, respectively. For these samples the standardized variable Z given in equation (3) equals 4.526. This value is outside the range between −2.58 and 2.58, and thus the change in the global mean is statistically significant at a 1% level. Even though both changes in means are statistically significant, there is more confidence in the change of the O-F mean because the variable Z in this case has a larger magnitude.

[20] Next, we explore the impact of changes in observation error characteristics on the assimilated fields. Two different sets of SBUV/2 calibration coefficients were used in producing the SBUV/2 data in April 2000 (following mark "A" in Figure 2). The impact of these calibration coefficients on the assimilated fields is seen in Figure 4. Both analyses were compared with independent WMO ozone sonde data for the period from April 1 to April 10, 2000. There is a very small change in the mean profile. The means of the analyses are not different at 5% significance level at any of the pressure levels shown. The RMS differences between sondes and the analysis with reprocessed SBUV/2 data are slightly smaller between 10 and 30 hPa,
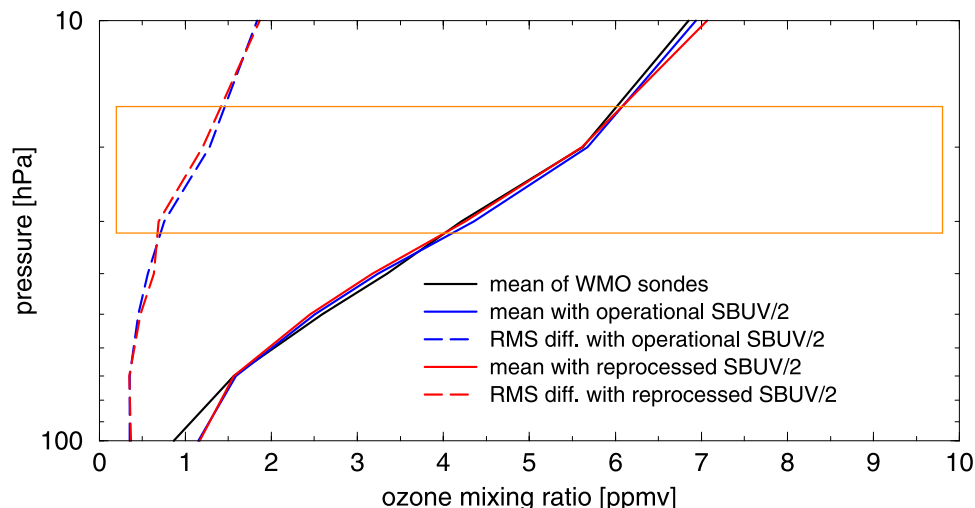
Figure 4. Comparison of the analyses with operational SBUV/2 ozone (blue) and the reprocessed SBUV/2 ozone (red) against independent WMO ozonesonde data (black) is given for April 1–10, 2000. The means of ozonesonde profiles and collocated analyses are shown by solid lines. The RMS differences between sondes and each of the analyses are shown by dashed lines. Umkehr layer 5 (16 to 32 hPa) is marked by the orange box. In this layer there is a small improvement in the agreement between sondes and assimilation when reprocessed SBUV/2 data are used. This is consistent with the lower mean of O-F residuals with reprocessed SBUV/2 data following mark "A" in Figure 2.

and slightly larger near 40 hPa, than for the analysis with the operational SBUV/2 ozone. The comparison against HALOE data was done using ~290 profiles in the Tropics and southern middle latitudes during the first 10 days in April 2000. This comparison also shows a very small impact from the change in the SBUV/2 data on the quality of the analyzed ozone. During the same period, we compared the assimilated ozone against POAM data [*Lumpe et al.*, 2002] near 65°N and found a small impact, but a slightly improved mean profile shape with the reprocessed SBUV/2 data. The RMS differences for the analysis with reprocessed SBUV/2 data are smaller between 3 and 10 hPa, and at 30 hPa, and larger elsewhere in the profile. Overall in comparisons with ozone sonde, HALOE and POAM data, we found that there was a very subtle impact on the assimilated ozone from the SBUV/2 calibration change on March 31, 2000. The changes in the assimilated ozone fields are much less pronounced than the change in the O-F statistics (near mark "A" in Figure 2).

[21] The NOAA 14 SBUV-2 instrument experienced grating position changes during November 2000 (see change in O-F statistics between marks "B" and "C" in Figure 2). We examine the impact of these grating position changes on the quality of the analyzed ozone field (Figure 5). The mean difference between assimilated ozone and independent POAM profiles in southern high latitudes is shown for November 13 to 30 (dashed line) and for December of 2000 (solid line). The comparison in November was done against 121 POAM profiles that cover between 70°S and 66°S. In December, 212 POAM profiles were used in the latitudes between 66°S and 63°S. Unfortunately, POAM data sample different latitudes at different times and thus in this comparison we need to consider the underlying geophysical variability. In order to minimize its effects we restrict the comparison to data from consecutive months, and within the 7° wide latitude band. This latitude

band that is covered by POAM is also observed by SBUV/2 data during November and December. A noticeably better agreement between POAM and assimilation is seen during December between 5 and 30 hPa, except at 20 hPa. The
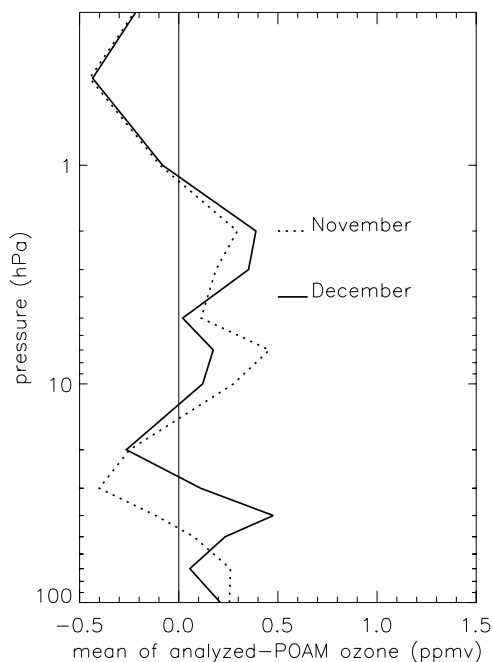
Figure 5. Comparison of mean differences between assimilated ozone mixing ratio and independent POAM ozone profiles in southern high latitudes is shown for November 13–30 and for December 2000. There is an improvement in the quality of assimilated ozone in the middle stratosphere in December, which is consistent with the decrease of the mean O-F residuals between November and December seen in Figure 2.
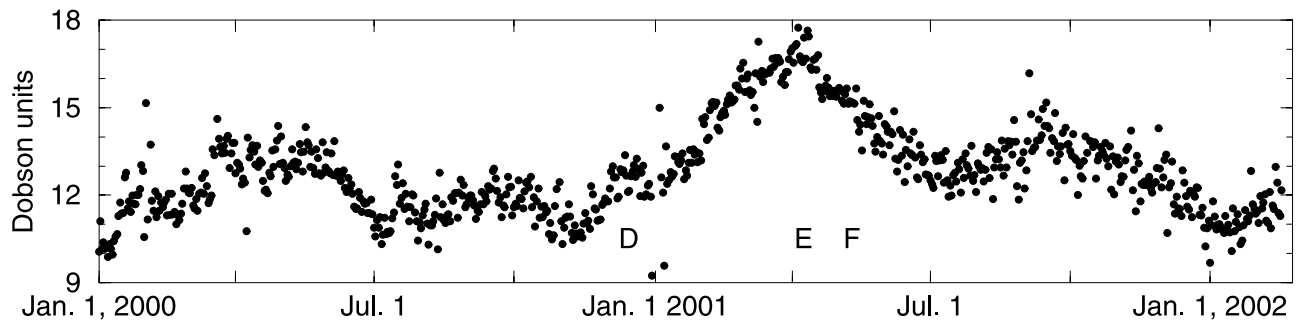
Figure 6. Time series of daily global RMS of total column ozone O-F residuals is shown. See text for details about marks "D" – "F". It shows a typical annual cycle during the year 2000. Following the mark "D" the RMS increases due to TOMS cross-track bias and the decrease in NOAA 14 SBUV/2 coverage. After switching to the use of NOAA 16 SBUV/2 profiles (mark "E") and total columns (mark "F"), the RMS decreases to near the levels seen in year 2000.

means differ at 5% significance level on all pressure levels between 5 and 70 hPa, except at 20 hPa. In addition, the means differ at 1% significance level on pressure levels of 3, 7, 10, 30, 40, 50, and 70 hPa. The integrated difference between analysis and POAM in the layer 16–32 hPa decreased in December, primarily due to a reversal of the sign of the mean difference at 30 hPa. In order to examine geophysical significance of this change, we compare its size with spatial and temporal changes of the ozone mean in this region and period in the Upper Atmosphere Research Satellite extended ozone climatology (available on the World Wide Web at http://code916.gsfc.nasa.gov/Public/Analysis/UARS/uarp/home.html). The climatological ozone means at 31.6 hPa change by ∼0.1 ppmv between 64°S and 68°S, and they change by ∼0.01 ppmv between November and December at these latitudes. Both of these changes are smaller than the change in the mean difference between analysis and POAM at 30 hPa of ∼0.5 ppmv (Figure 5). The improvement in the mean difference between analysis and POAM at 30 hPa is consistent with the improvement in the mean of O-F residuals (for the layer between 16 and 32 hPa) seen past mark "C" in Figure 2.

3.4. Concluding Remarks of Section 3

[22] The above two examples of SBUV/2 calibration and instrument changes show that the statistics of O-F residuals from an assimilation system are indeed very sensitive to changes in the observations and their error characteristics. Furthermore, these statistics are collected in near-real time, and allow a rapid feedback to the instrument team. They are also robust over systems driven by different meteorological data, and including or excluding the effects of the chemical processes. In contrast to the sensitivity of O-F residuals, the change in the assimilated ozone on March 31, 2000 was very subtle, and hard to detect from comparisons with independent high quality data (sondes, POAM, and HALOE). However, during the SBUV/2 instrument grating position changes in November 2000, both the mean O-F residuals and the agreement between assimilated ozone and POAM data were notably degraded.

4. Total Ozone Column Data

[23] In this section we examine several properties of the total column ozone O-F residuals: their annual variability,

their use for detection of cross-track biases of the scanning TOMS instrument, and their changes due to a switch to another source of total column ozone data (NOAA 16 SBUV/2). Finally, we study the sensitivity of the ozone O-F residuals to changes in the meteorological assimilation system whose winds are used to drive the ozone assimilation model.

4.1. Earth Probe Total Ozone Mapping Spectrometer Total Ozone Column Data

[24] An example of the time series of the global daily RMS of total column ozone O-F residuals is shown in Figure 6. We focus first on the day-to-day variability seen in this time series. In 24 hours TOMS normally provides near-global coverage of the sunlit portion of the Earth. Abrupt short-term changes in Figure 6 are typically caused by a reduced coverage of total ozone observations. For example, this occurs when total ozone data file is not available on time for the operational analysis. The only total column data that are available are then those from the end of the last orbit that started on the previous day because they are contained in the data file for the previous day. This happened on December 30, 2000 when we used only a part of one orbit going from southern high latitudes to the equator. In this region the ozone field has lower values and lower variability than in the northern middle latitudes. Therefore the RMS of O-F residuals for all observations on this day is ∼9.2 DU, which is well below the usual range of RMS values in December 2000 of ∼12 to 13 DU. The total ozone data were not available for almost 5 days. When the data returned on January 4 the O-F differences are larger (the RMS value is almost 15 DU) because of the accumulation of model errors over the 5 days for which total ozone column data were not available. The RMS of O-F residuals returns to near 12 DU within one to two days after the TOMS data become available.

[25] A typical seasonal cycle is seen in Figure 6 during the year 2000. The global RMS of total ozone O-F residuals is the lowest in January during the northern winter, when the northern high latitudes are in the polar night, unobserved by TOMS, and do not contribute to the global statistics. This RMS value peaks during the northern spring when ozone values increase, and the dynamical variability is large, especially in the northern middle and high latitudes which are both observed by TOMS. The RMS value then
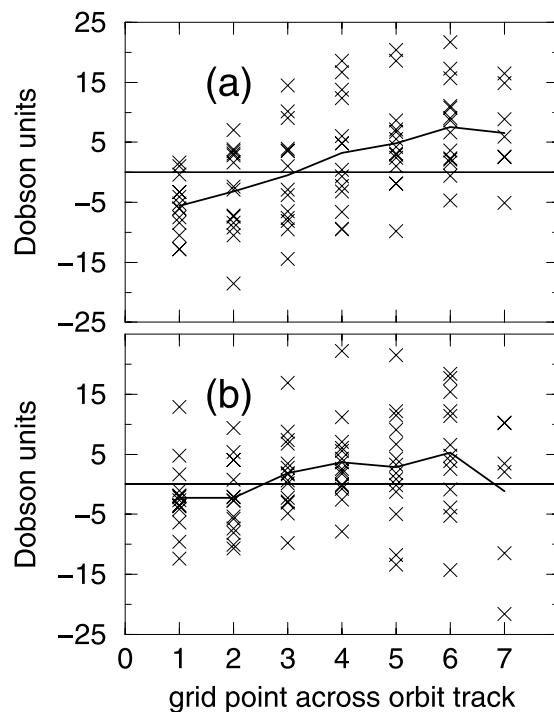
Figure 7. EP TOMS O-F residuals at 2° south latitude are shown by crosses as a function of the grid point across the orbit track. The westmost grid point is 1 and the eastmost is 7. The mean of O-F residuals for each grid point is shown by the line. The residuals and their mean are shown on January 28 of the year 2001 in Figure 7a and year 2000 in Figure 7b.

falls until July, and rises again until October. The increase in the RMS of total ozone O-F residuals during northern hemisphere winter and spring (January to April) is larger in magnitude than that corresponding to the southern hemisphere winter and spring (July to October).

[26] Starting in year 2000 the near-real time retrieved total column ozone from EP TOMS began developing a cross-track bias that grew over time and degraded the quality of the data. According to the TOMS processing team the bias appears to be due to a change in the optical properties of the front scan mirror of the instrument (news release on November 15, 2001 at http://toms.gsfc.nasa.gov/news/news.html). This cross-track bias is illustrated by the scatterplot in Figure 7a. The TOMS O-F residuals at 2°S (where the geophysical variability in the total column ozone field is relatively small, except for the zonal wave number one) are shown by crosses for 14 orbits on January 28, 2001. The O-F residuals are plotted versus the model grid point across the orbit, where 1 denotes the westmost and 7 the eastmost grid point. The mean of O-F residuals for each of the grid points is shown by a line, and it increases from west to east by 13.1 Dobson units (DU). A year earlier, on January 28, 2000 the TOMS cross-track bias was smaller (Figure 7b) and the mean of O-F residuals for 14 orbits had a smaller variability of 7.6 DU. In addition, the means were computed for ten days (January 20 to 29) in years 2000 and 2001, and the cross-track change in the means increased from <3 DU in year 2000 to more than 10 DU in year 2001.

[27] A departure from the typical seasonal cycle is visible from November of 2000 (just preceding mark "D" in Figure 6). A strong upward trend begins and culminates with the peak in April 2001 (mark "E"). This increase is larger than that of a typical seasonal cycle. It was due to both the degradation of the quality of EP TOMS and a drift of the NOAA 14 orbit. The drift of the NOAA 14 orbit toward a later afternoon Equator crossing caused a decrease of the SBUV/2 spatial coverage, an increase in the solar zenith angles of the measurements, and a consequent degradation of the ozone products (L. Flynn, personal communication, 2001). In April 2001 (mark "E" in Figure 6) we started assimilating NOAA 16 instead of NOAA 14 SBUV/2 profile data. The RMS of O-F residuals started decreasing as the ozone profiles became better constrained by the NOAA 16 SBUV/2 observations with higher quality and better coverage than those from the NOAA 14 instrument. Since May 2001 (mark "F" in Figure 6) total column ozone data from NOAA 16 SBUV/2 have been assimilated instead of those from EP TOMS. This slightly increased the day-to-day scatter of the RMS of the O-F residuals, but in January 2002 they returned to values similar to those of January 2000.

[28] The time series of zonal RMS differences between total column ozone observations and the forecast is shown in Figure 8. Lower values are typically found in the Tropics where both the total column ozone amounts and their
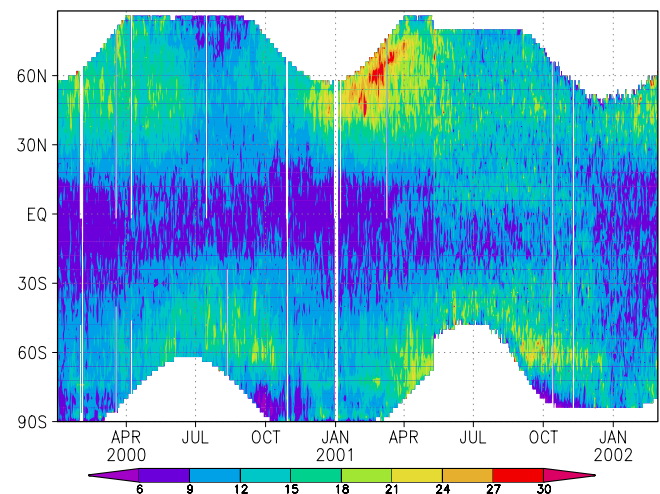
Figure 8. Time series of the zonal RMS difference between total column observations and the forecast from the near-real time ozone assimilation system (in Dobson units) is shown. A typical distribution is seen in year 2000: the lowest RMS differences are within the "ozone hole" region (in the high southern latitudes in September and October), relatively low differences are in the Tropics, and the highest differences are in middle to high latitudes during springtime in both hemispheres. A buildup in the RMS differences is seen from about December 2000 to May 2001. The abrupt reduction in the latitudinal coverage of the total column ozone data in May 2001 occurs because the source of total column ozone data was changed from EP TOMS to NOAA 16 SBUV/2. White areas indicate that data were not available for a specific time and latitude, e.g., within the polar night, or when a data file is missing for a day.

spatio-temporal variability are lower than in extratropics. The RMS differences and the ozone amounts are lower only inside the Antarctic "ozone hole" which is seen in the southern high latitudes around October. The RMS differences are typically higher in middle latitudes, especially in winter and spring when total ozone amounts as well as their dynamical variability increase. Note that most of the build-up in the global RMS of total ozone O-F residuals (seen between marks "D" and "E" in Figure 6) begins in northern middle latitudes in December 2000, extends to northern high latitudes in February 2001, and another buildup is seen in southern high latitudes around April 2001.

4.2. NOAA 16 SBUV/2 Total Ozone Column Data

[29] During May 2001, when the ozone assimilation system started using NOAA 16 SBUV/2 total column ozone data instead of EP TOMS data, an abrupt change occurs in spatial coverage (Figure 8): the latitudinal coverage decreases by ~5° in the northern hemisphere, and by ~15° in the southern hemisphere. After several days of the initial adjustment of the system to the total column data from NOAA 16 SBUV/2, the RMS differences in the northern middle and high latitudes decrease. The RMS in the southern middle latitudes increases as expected from the previous annual cycle. The RMS values in the southern Tropics are just slightly higher than those seen in the year 2000 when the TOMS data were assimilated. However, the RMS values in the northern tropics between May and December of year 2001 are higher than during previous periods. The SBUV/2 instrument provides measurements at nadir points only, for ~14 orbits per day. In contrast, EP TOMS is a scanning instrument that provides almost complete coverage of the Tropics every day. About 10,000 total column observations were used daily from EP TOMS, compared to ~900 observations from NOAA 16 SBUV/2. The observation error standard deviation used for SBUV total ozone is 3% of the observed value. The SBUV footprint is comparable to the model grid cell, so the representativeness error is not modeled. For TOMS total ozone the observation error variance is the sum of the squares of two terms: the measurement and retrieval error standard deviation, which is 1.5% of the observed value, and the representativeness error standard deviation, which typically ranges between 3 and 7 DU [*Stajner et al.*, 2001]. With sparser total column ozone data from SBUV/2, and often higher observation errors, the forecast relies more heavily on the model, and the forecast errors explain a larger portion of the O-F residuals.

4.3. Changes in the Meteorological System

[30] The zonal RMS of O-F residuals (in Figure 8, especially in the Tropics) and the zonal mean of O-F residuals (not shown) decrease in December 2001 following several simultaneous changes in the meteorological GEOS-3 assimilation system. One of the changes in the meteorological system was the use of in-house TOVS retrievals, including moisture data, instead of NESDIS TOVS retrievals. Another change was made to the radiation package of the general circulation model, to parameterize the effects of trace gasses. Assimilation of total precipitable water and the land-surface emissivities were also modified. The wind analysis

increments were constrained so that the vertically averaged velocity potential vanishes. Forecast error variances were changed to be uniform on each level. However, all these changes to the meteorological system were introduced simultaneously, and it is not clear which ones had the largest effect on the ozone transport.

4.4. Discussion

[31] We found that the total column ozone O-F residuals are sensitive to instrument cross-track biases. The size of O-F residuals changes with a switch in the instrument whose total column data are used. The O-F residuals are also sensitive to changes in the meteorological system used to produce winds that drive ozone transport in the ozone assimilation system. Thus the ozone O-F residuals can be used for indirect evaluation of the transport properties of assimilated winds, especially in the stratosphere, which contains the most of the ozone column.

5. NOAA 16 SBUV/2 Ozone Profiles

[32] The NOAA 16 SBUV/2 instrument became operational in early 2001. This first year of operations provides an interesting period for evaluating changes in the error characteristics of the retrieved ozone data. During this period the instrument characteristics become better known and frequently some modifications are made to instrument calibration and to the retrieval algorithm. We will show how these changes are detected in assimilation and how they affect the assimilated ozone field.

[33] Daily monitoring of the NOAA 16 SBUV/2 O-F residual regional statistics was implemented in May 2001. In the next example we focus on the SBUV observations in the Umkehr layer 7, between ~4 and 8 hPa. There is ~20–25 DU of ozone in this layer and the spatial standard deviation is ~3–4 DU. The mean of the O-F residuals in the northern middle latitudes for this layer is shown in Figure 9 (lower curve, labeled by "UL 7 mean"). Larger than typical variability can be seen in May, around October 9 and 13, and December 6. The change on October 13 was caused by the unintended use of NOAA 14 instead of NOAA 16 SBUV/2 data in the assimilation, and the bias between these two SBUV/2 data sets. Each of the other three jumps in the O-F statistics coincides with a change in either instrument calibration or in the operational retrieval algorithm used to produce NOAA 16 SBUV ozone data: the photomultiplier tube temperature correction was changed in the retrieval algorithm in May, the calibration was changed to use automatic inter-range ratio update using on-orbit data instead of extrapolated time dependent table on October 9, and finally in December the calibration started using new time dependent albedo correction factors and the retrieval algorithm for pressure mixing of ozone estimates for different wavelength pairs was modified (S. Kondragunta, personal communication, 2001).

[34] One convenient statistic for monitoring of the changes in the O-F residuals is z/p (for z from equation (2)), the mean of χ^2 statistics normalized by the number of observations. Recall that under the ideal conditions its value should be one. This statistic accounts for all the O-F residuals according to their error covariances. It provides one global number representing all residuals from different regions,
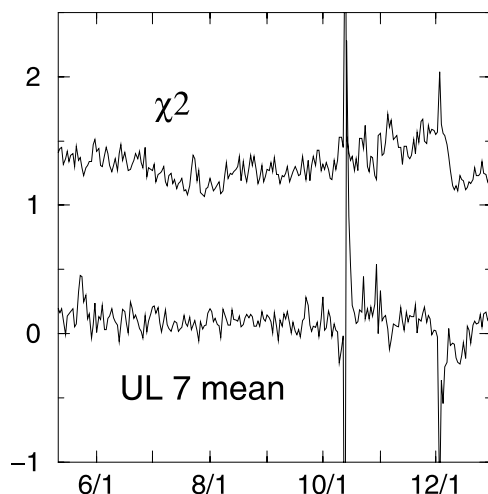
Figure 9. Time series of the daily mean of the global χ^2 statistic normalized by the total number of observations is shown (upper curve, labeled "χ^2") from May to December 2001. An example of a regional O-F statistic is shown by the lower curve (labeled by "UL 7 mean"). It is the time series of the mean of O-F residuals (in Dobson units) in northern middle latitudes for the NOAA 16 SBUV/2 ozone in Umkehr layer 7 between $\sim$4 and 8 hPa. There is a close correspondence between the jumps in the two time series, which exceed the typical day-to-day variability, e.g., in May, October, and December.

levels, and observing conditions. *Ménard et al.* [2000] and *Ménard and Chang* [2000] relied on χ^2 statistics for estimation of error covariance model parameters in a constituent data assimilation system. In our experience, χ^2 is sensitive to changes in observation error characteristics for all the regions: it thus serves as an initial monitor of sudden changes, which prompt searches to determine the region where the changes occurred by inspecting mean and RMS statistics for different regions and levels. The time series of realizations of χ^2 statistics from our system is shown in Figure 9 by the upper curve (labeled by "χ^2"). For each of the large sudden changes in the mean of O-F residuals in the layer 4–8 hPa (Figure 9, lower curve, labeled by "UL 7 mean") there is a corresponding sudden change in the time series of the χ^2 statistics.

[35] Next, we compare the quality of assimilated ozone before and after the jump in χ^2 in the beginning of December 2001. A comparison of assimilated ozone with HALOE data is shown in Figure 10. The mean differences between assimilation and HALOE data are shown for the second half of December 2001 (solid curves) and for November 2001 (dashed curves). The comparison is shown for all the regions (Tropics, northern and southern middle latitudes, and southern high latitudes) for which HALOE data are available. Despite the inherent differences in HALOE sampling, we found that the agreement between the assimilated ozone and HALOE is generally improved in all these regions after the SBUV/2 calibration and algorithm change on December 4. The largest improvement is seen in the upper stratosphere. In all regions the means are different at 1% significance level at pressure levels of 1 and 5 hPa. These improvements in the analysis mean are consistent

with the improvement in the normalized mean of χ^2 statistics seen from about December 10 in Figure 9.

6. Discussion and Future Work

[36] The monitoring of statistics of O-F residuals in an assimilation system was shown to be a sensitive procedure for detecting changes in the error characteristics of ozone observations from satellite-borne sensors. These monitoring results were demonstrated to be robust to use of different assimilating models, such as transport driven by GEOS-3 or GEOS-4 winds, and inclusion or exclusion of a parameterized chemistry scheme. We illustrated through several examples that the monitoring through assimilation is a potentially effective method for detecting changes in the errors of satellite ozone data. Time-dependent changes in the observation error characteristics of NOAA 14 SBUV/2, NOAA 16 SBUV/2, and EP TOMS instruments were detected. In the case of the NOAA 14 calibration change, we found an increase in the O-F residuals. Following this finding the SBUV/2 instrument team updated the calibration coefficients for the second time, we assisted in the validation of these updated calibration coefficients, and these coefficients were later implemented by NOAA in the operational processing of NOAA 14 SBUV/2 data.

[37] Comparisons of assimilated ozone fields with independent high-quality observations (from ozone sondes, HALOE, and POAM) indicate that the mean and RMS statistics of O-F residuals are very sensitive to changes in the input data quality. A noticeable change in O-F statistics corresponds to a subtle change in the quality of analyzed ozone fields in the case of NOAA 14 SBUV/2 calibration modification in March of year 2000. In contrast, the increase of O-F residuals during November 2000 when NOAA 14 SBUV/2 experienced grating position anomalies is coincident with a clear degradation in the quality of assimilated ozone in the comparison with POAM data. Another case indicates the importance of χ^2 statistic. The improvement in the values of normalized mean of χ^2 statistic during December 2001 was coincident with the improvement in the quality of assimilated NOAA 16 SBUV/2 ozone, which was evaluated through comparison with HALOE data.

[38] Commonly used assumptions about unbiased observation and forecast errors in the assimilation are likely to cause partial propagation of the forecast and/or observation biases into assimilated fields. This limits the accuracy of the current operational assimilated ozone. Before interpreting changes in the ozone field as geophysically significant, their further validation is necessary. One approach is to compare the assimilated fields with independent observations. Inspection of the O-F statistics is also helpful. Our experience indicates that the most convenient statistics whose time series should be inspected is the mean of χ^2 normalized by the number of observations. When changes are found we proceed to an inspection of regional statistic of O-F residuals.

[39] Environmental monitoring relies on the use of model-assimilated observations from many data sources. A synthesis of all observational data with prediction models through statistical assimilation techniques, provides the only means possible of estimating consistent, multivariate fields
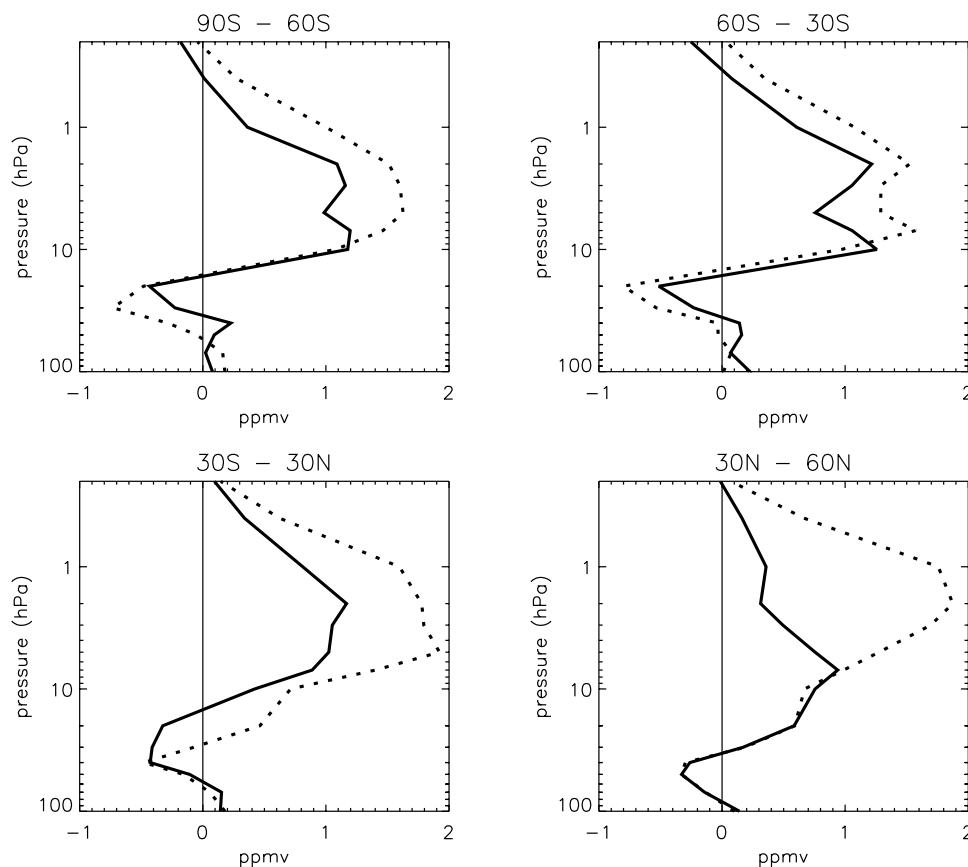
Figure 10. Regional mean differences between analyzed ozone and HALOE data before (dashed) and after (solid) the calibration and algorithm change in NOAA 16 SBUV/2 retrievals on December 4, 2001 are shown. Following the change in the retrievals there is generally an improvement in the quality of the assimilated ozone profile, especially at pressures <10 hPa.

of environmental parameters [*National Research Council*, 1991]. This synthesis is typically done in two ways: operationally in near-real time using different, ever improving models, and in the "reanalysis" framework where a fixed state-of-the-art model and a fixed statistical assimilation technique are used over an extended historical period [*Schubert et al.*, 1993; *Kalnay et al.*, 1996; *Gibson et al.*, 1997; *Simmons and Gibson*, 2000]. Both types of synthesis are affected by inevitable discontinuities between instruments or even the types of environmental observations that are available for usage.

[40] The validation statistics presented in this study contain some results applicable to reanalyses, while others are relevant only to "real-time" operational monitoring. Examples of the latter are changes in ozone forecast model brought about by the meteorological analyses (changes in GEOS-3 in December 2001) and by the combination of introducing a parameterized ozone chemistry model at the same time as changing from GEOS-3 to GEOS-4 analyses (the "reanalysis" shown in Figure 2). The most important issues for reanalysis pertain to the unavoidable changes in instruments and to the time dependence of the data quality from any one instrument. Two important effects, the degradation of EP-TOMS data quality and the effective loss of NOAA 14 SBUV/2 data caused by the orbital drift, had marked impacts on the quality of the resultant ozone analyses, clearly characterized by the long-term behavior

of the monitoring statistics. For reanalysis purposes, these effects must be considered.

[41] In a near-real time system, the re-calibration of SBUV/2 retrievals had an impact on analysis quality, an effect not immediately obvious from the analyses, but clearly evident in the O-F residuals. Effects such as these, which can also be detected by careful monitoring of the retrieved data without assimilation, are crucial to the success and realism of analyses. The fundamental point about that analysis is not that assimilation can detect changes in the retrieval algorithms (these should be known anyway): it is that assimilation can isolate the impacts of such changes and, in the context of an end-to-end environmental monitoring system, can provide quantitative measures of these impacts and offer guidance into producing more appropriate changes that lead to a smaller shock to the system. The underlying message of this work is that careful use of the monitoring statistics, alongside the assimilated products, can yield a beneficial insight into the quality of the data and the suitability of any long-term analyses for inferring global change through quantitative, robust measures of the model-data uncertainty.

[42] Several instruments that measure ozone are included on the recent and planned satellites: Earth Observing System (EOS) Aqua, EOS Aura, and Environmental Satellite (Envisat). We have already applied the monitoring through assimilation for ozone observations from Envisat,

from the AIRS instrument on EOS Aqua, and from the Microwave Limb Sounder onboard NASA's Upper Atmosphere Research Satellite. We plan to extend the monitoring through assimilation to retrieved ozone data from instruments on EOS Aura.

References

Atlas, R., S. C. Bloom, R. N. Hoffman, E. Brin, J. Ardizzone, J. Terry, D. Bungato, and J. C. Jusem (1999), Geophysical validation of NSCAT winds using atmospheric data and analyses, *J. Geophys. Res.*, 104, 11,405–11,424.

Aumann, H. H., et al. (2003), AIRS/AMSU/HSB on the Aqua mission: Design, science objectives, data products, and processing systems, *IEEE Trans. Geosci. Remote Sens.*, 41, 253–264.

Austin, J. (1992), Toward the four dimensional assimilation of stratospheric constituents, *J. Geophys. Res.*, 97, 2569–2588.

Bhartia, P. K., R. D. McPeters, C. L. Mateer, L. E. Flynn, and C. Wellemeyer (1996), Algorithm for the estimation of vertical ozone profile from the backscattered ultraviolet (BUV) technique, *J. Geophys. Res.*, 101, 18,793–18,806.

Brühl, C., et al. (1996), HALOE Ozone Channel Validation, *J. Geophys. Res.*, 101, 10,217–10,240.

Daley, R. (1991), *Atmospheric Data Analysis*, Cambridge Univ. Press, New York.

Dethof, A., and E. Holm (2002), Ozone in ERA-40: 1991–1996, *ECMWF Tech. Memo.*, 377, 31 pp.

Elbern, H., and H. Schmidt (2001), Ozone episode analysis by four-dimensional variational chemistry data assimilation, *J. Geophys. Res.*, 106, 3569–3590.

Eskes, H. J., A. J. M. Piters, P. F. Levelt, M. A. F. Allaart, and H. M. Kelder (1999), Variational assimilation of GOME total-column ozone satellite data in a 2 D latitude-longitude tracer-transport model, *J. Atmos. Sci.*, 56, 3560–3572.

Eskes, H. J., P. F. J. van Velthoven, P. J. M. Valks, and H. M. Kelder (2003), Assimilation of GOME total ozone satellite observations in a three-dimensional tracer transport model, *Q. J. R. Meteorol. Soc.*, 129, 1663–1681.

Fetzer, E., et al. (2003), AIRS/AMSU/HSB validation, *IEEE Trans. Geosci. Remote Sens.*, 41, 418–431.

Fisher, M., and D. J. Lary (1995), Lagrangian four-dimensional variational data assimilation of chemical species, *Q. J. R. Meteorol. Soc.*, 131, 1681–1704.

Fleming, E. L., C. H. Jackman, D. B. Considine, and R. S. Stolarski (2001), Sensitivity of tracers and a stratospheric aircraft perturbation to two-dimensional model transport variations, *J. Geophys. Res.*, 106, 14,245–14,263.

Froidevaux, L., et al. (1996), Validation of UARS Microwave Limb Sounder ozone measurements, *J. Geophys. Res.*, 101, 10,017–10,060.

Gibson, J. K., P. Kållberg, S. Uppala, A. Nomura, A. Hernandez, and E. Serrano (1997), ERA Description. *ECMWF Reanal. Final Rep. Ser.*, 1, 71 pp.

Gille, J. C., et al. (1996), Accuracy and precision of Cryogenic Limb Array Etalon Spectrometer (CLAES) temperature retrievals, *J. Geophys. Res.*, 101, 9583–9602.

Hollingsworth, A., D. B. Shaw, P. Lonnberg, L. Illari, K. Arpe, and A. J. Simmons (1986), Monitoring of observation and analysis quality by a data assimilation system, *Mon. Wea. Rev.*, 114, 861–879.

Hollingsworth, A., P. Viterbo, and A. J. Simmons (2003), The relevance of numerical weather prediction for forecasting natural hazards and for monitoring the global environment, in *A Half Century of Progress in Meteorology: A Tribute to Richard J. Reed*, edited by R. H. Johnson and R. A. Houze Jr., pp. 109–129, Am. Meteorol. Soc., Boston, Mass.

Kalnay, E., et al. (1996), The NCEP/NCAR 40-year reanalysis project, *Bull. Am. Meteorol. Soc.*, 77, 437–471.

Khattatov, B. V., J.-F. Lamarque, L. V. Lyjak, R. Menard, P. F. Levelt, X. X. Tie, G. P. Brasseur, and J. C. Gille (2000), Assimilation of satellite observations of long-lived chemical species in global chemistry-transport models, *J. Geophys. Res.*, 105, 29,135–29,144.

Langematz, U. (2000), An estimate of the impact of observed ozone losses on stratospheric temperature, *Geophys. Res. Lett.*, 27, 2077–2080.

Levelt, P. F., B. V. Khattatov, J. C. Gille, G. P. Brasseur, X. X. Tie, and J. W. Waters (1998), Assimilation of MLS ozone measurements in the global three-dimensional chemistry transport model ROSE, *Geophys. Res. Lett.*, 25, 4493–4496.

Lin, S.-J., and R. B. Rood (1996), Multidimensionsl flux-form semi-langrangian transport schemes, *Mon, Wea. Rev.*, 124, 2046–2070.

Long, C. S., A. J. Miller, H. T. Lee, J. D. Wild, R. C. Przywarty, and D. Hufford (1996), Ultraviolet index forecasts issued by the National Weather Service, *Bull. Am. Meteorol. Soc.*, 77, 729–748.

Lumpe, J. D., R. M. Bevilacqua, K. W. Hoppel, and C. E. Randall (2002), POAM III retrieval algorithm and error analysis, *J. Geophys. Res.*, 107(D21), 4575, doi:10.1029/2002JD002137.

McPeters, R. D., et al. (1998), *Earth Probe Total Ozone Mapping Spectrometer (TOMS) Data Products User's Guide, NASA Tech. Publ. 1998-206895*, NASA, Washington, D. C.

Ménard, R., and L.-P. Chang (2000), Assimilation of stratospheric chemical tracer observations using a Kalman filter, Part II: χ^2-validated results and analysis of variance and correlation dynamics, *Mon. Wea. Rev.*, 128, 2672–2686.

Ménard, R., S. E. Cohn, L.-P. Chang, and P. M. Lyster (2000), Assimilation of stratospheric chemical tracer observations using a Kalman filter. Part I: Formulation, *Mon. Wea. Rev.*, 128, 2654–2671.

National Research Council (1991), *Four-Dimensional Model Assimilation of Data: A Strategy for the Earth System Sciences*, Natl. Acad. Press, Washington, D. C.

Piters, A. J. M., P. F. Levelt, M. A. F. Allaart, and H. M. Kelder (1999), Validation of GOME total ozone column with the Assimilation Model KNMI, *Remote Sensing: Earth, Ocean and Atmosphere*, 22, 1501–1504.

Remsberg, E., et al. (2002), An assessment of the quality of Halogen Occultation Experiment temperature profiles in themesosphere based on comparisons with Rayleigh backscatter lidar and inflatable falling sphere measurements, *J. Geophys. Res.*, 107(D20), 4447, doi:10.1029/2001JD001521.

Riishøjgaard, L. P., I. Stajner, and G.-P. Lou (2000), The GEOS ozone data assimilation system, *Adv. Space Res.*, 25, 1063–1072.

Rodgers, C. D., and B. J. Connor (2003), Intercomparison of remote sounding instruments, *J. Geophys. Res.*, 108(D3), 4116, doi:10.1029/2002JD002299.

Schubert, S. D., R. B. Rood, and J. Pfaentner (1993), An assimilated dataset for Earth science applications, *Bull. Am. Meteorol. Soc.*, 77, 437–471.

Simmons, A. J., and J. K. Gibson (2000), The ERA-40 project plan, *Era-40 Proj. Rep. Ser.*, 1, 63 pp.

Smith, W. L., H. M. Woolf, C. M. Hayden, D. Q. Wark, and L. M. McMillin (1979), The TIROS-N operational vertical sounder, *Bull. Am. Meteorol. Soc.*, 60, 1177–1187.

Spiegel, M. R. (1975), *Schaum's Outline of Theory and Problems of Probability and Statistics*, McGraw-Hill, New York.

Stajner, I., L. P. Riishøjgaard, and R. B. Rood (2001), The GEOS ozone data assimilation system: Specification of error statistics, *Q. J. R. Meteorol. Soc.*, 127, 1069–1094.

Stoffelen, A. (1999), A simple method for calibration of a scatterometer over the ocean, *J. Atmos. Ocean Tech.*, 16, 275–282.

Struthers, H., R. Brugge, W. A. Lahoz, A. O'Neill, and R. Swinbank (2002), Assimilation of ozone profiles and total column measurements into a global general circulation model, *J. Geophys. Res.*, 107, 4438, doi:10.1029/2001JD000957.

Uppala, S. (1997), Observing system performance in ERA, *ECMWF Reanal. Proj. Rep. Ser., 3*, 261 pp.

S. Pawson, R. Rood, I. Stajner, and N. Winslow, Global Modeling and Assimilation Office, Code 900.3, NASA Goddard Space Flight Center, Greenbelt, MD 20771, USA. (spawson@gmao.gsfc.nasa.gov; rrood@gmao.gsfc.nasa.gov; istajner@gmao.gsfc.nasa.gov; nwinslow@gmao.gsfc.nasa.gov)